

About the
consistency between
Envisat and
CryoSat-2 radar
freeboard retrieval

S. Schwegmann et al.

About the consistency between Envisat and CryoSat-2 radar freeboard retrieval over Antarctic sea ice

S. Schwegmann¹, E. Rinne², R. Ricker¹, S. Hendricks¹, and V. Helm¹

¹Alfred Wegener Institute, Helmholtz-Centre for Polar- and Marine Research, Am Handelshafen 12, 27570 Bremerhaven, Germany

²Finnish Meteorological Institute, Marine Research, Erik Palménin aukio 1, 00560, Helsinki, Finland

Received: 26 June 2015 – Accepted: 7 August 2015 – Published: 16 September 2015

Correspondence to: S. Schwegmann (sandra.schwegmann@awi.de)

Published by Copernicus Publications on behalf of the European Geosciences Union.

Title Page

Abstract

Introduction

Conclusions

References

Tables

Figures

◀

▶

◀

▶

Back

Close

Full Screen / Esc

Printer-friendly Version

Interactive Discussion

Abstract

Knowledge about Antarctic sea-ice volume and its changes over the past decades has been sparse due to the lack of systematic sea-ice thickness measurements in this remote area. Recently, first attempts have been made to develop a sea-ice thickness product over the Southern Ocean from space-borne radar altimetry and results look promising. Today, more than 20 years of radar altimeter data are potentially available for such products. However, data come from different sources, and the characteristics of individual sensors differ. Hence, it is important to study the consistency between single sensors in order to develop long and consistent time series over the potentially available measurement period. Here, the consistency between freeboard measurements of the Radar Altimeter 2 on-board Envisat and freeboard measurements from the Synthetic-Aperture Interferometric Radar Altimeter on-board CryoSat-2 is tested for their overlap period in 2011. Results indicate that mean and modal values are comparable over the sea-ice growth season (May–October) and partly also beyond. In general, Envisat data shows higher freeboards in the seasonal ice zone while CryoSat-2 freeboards are higher in the perennial ice zone and near the coasts. This has consequences for the agreement in individual sectors of the Southern Ocean, where one or the other ice class may dominate. Nevertheless, over the growth season, mean freeboard for the entire (regional separated) Southern Ocean differs generally by not more than 2 cm (5 cm, except for the Amundsen/Bellingshausen Sea) between Envisat and CryoSat-2, and the differences between modal freeboard lie generally within ± 10 cm and often even below.

1 Introduction

Over the last three decades, sea-ice extent (SIE) in the Arctic has decreased and submarine ice draft measurements indicate that also sea-ice volume is declining (Rothrock et al., 1999, 2008; Lindsay and Schweiger, 2015). In the Antarctic on the contrary, SIE

TCD

9, 4893–4923, 2015

About the
consistency between
Envisat and
CryoSat-2 radar
freeboard retrieval

S. Schwegmann et al.

Title Page

Abstract

Introduction

Conclusions

References

Tables

Figures

◀

▶

◀

▶

Back

Close

Full Screen / Esc

Printer-friendly Version

Interactive Discussion



About the consistency between Envisat and CryoSat-2 radar freeboard retrieval

S. Schwegmann et al.

Title Page

Abstract

Introduction

Conclusions

References

Tables

Figures

◀

▶

◀

▶

Back

Close

Full Screen / Esc

Printer-friendly Version

Interactive Discussion

is increasing, but only little is known about the changes in the sea-ice volume. This is due to the lack of systematic sea-ice thickness measurements in this remote area. There are only few in situ data sets from upward looking sonars (only Weddell Sea, e.g. Harms et al., 2001; Behrendt et al., 2013), drillings (e.g., Lange and Eicken, 1991; Ozsoy-Cicek et al., 2013; Wadhams et al., 1987; Perovich et al., 2004), electromagnetic methods (Haas, 1998; Weissling et al., 2011; Haas et al., 2008) and airborne altimetry (e.g., Dierking, 1995; Leuschen et al., 2008). Those data are distributed unevenly in location, coverage and time and do not allow for the estimation of seasonal and inter-annual sea-ice volume changes. Only ship-based visual observations (ASPeCt, Worby et al., 2008) have been used for estimations of the seasonal variability in selected regions. Hence, in order to investigate current mass balance and feedback mechanisms of the entire Antarctic sea-ice zone we need sea-ice thickness retrievals from satellite sensors.

The capability of sea-ice thickness retrievals using satellite altimetry data has been demonstrated for Arctic and Antarctic sea ice (Ricker et al., 2014; Laxon et al., 2013; Kurtz et al., 2014; Zwally et al., 2008; Yi et al., 2011). The altimetry sea-ice thickness retrieval algorithm is based on estimations of freeboard, the height of the ice (ice freeboard) or snow surface (total or snow freeboard) above the local sea level. One fundamental requirement for freeboard retrieval is the estimation of sea surface height (SSH) from altimeter range data over leads between ice floes. The SSH along the satellite ground track forms the reference surface, where the residual of surface elevations over ice gives the freeboard. Sea-ice thickness is then calculated from freeboard using hydrostatic equilibrium equations, requiring estimates of the snow depth and densities of sea ice, snow and water. There are two categories of altimeters currently used for space-borne freeboard measurements: the Geoscience Laser Altimeter System (GLAS) on-board the Ice, Cloud and land Elevation Satellite (ICESat) measured the distance to the snow/ice surface, hence reveals snow freeboard. Radar altimeters like the Radar Altimeter 2 on-board Envisat or the Synthetic-Aperture Interferometric Radar Altimeter on-board CryoSat-2 (CS-2) are based on K_u -Band frequencies. Com-

**About the
consistency between
Envisat and
CryoSat-2 radar
freeboard retrieval**

S. Schwegmann et al.

Title Page

Abstract

Introduction

Conclusions

References

Tables

Figures

◀

▶

◀

▶

Back

Close

Full Screen / Esc

Printer-friendly Version

Interactive Discussion



pared to laser altimetry, radar altimeters have the advantage of not being influenced by cloud cover, but yield significantly larger surface footprints. Surface backscatter at K_u -Band frequencies were originally assumed to be dominated by the snow/ice interface, thus yielding ice freeboard. However, this assumption has been recently questioned by several publications (Willatt et al., 2010, 2011; Ricker et al., 2014; Kurtz et al., 2014; Price et al., 2015; Kwok, 2014).

Over sea ice in the Southern Ocean, Zwally et al. (2008) and Yi et al. (2011) provided a first estimate of snow freeboard and sea-ice thickness distribution and its seasonal evolution in the Weddell Sea using the laser altimeter data from ICESat. They found the highest snow freeboard and the thickest ice in the western Weddell Sea and a clear seasonal cycle of the snow freeboard with the highest values in summer (since all the thin ice is melted away) and lower values in the beginning of winter (due to massive formation of new ice). A comparison between field data and ICESat ground track in the Bellingshausen Sea showed a good agreement between both methods (Xie et al., 2011). Recently, Kern and Spreen (2015) estimated finally the potential uncertainty of sea-ice thicknesses derived from ICESat and AMSR-E snow depth, which range between 20 and 80%. They found that the highest impact comes from the applied SSH detection, but a reasonable alternative to that detection does not show a huge difference. At the same time as the first ICESat snow freeboard maps were developed by Zwally et al. (2008), Giles et al. (2008) computed freeboard out of radar altimeter data from the European Remote Sensing satellite 2 (ERS-2). In their study they could show that the winter mean freeboard from ERS-2 shows a reasonable distribution and good qualitative agreement with ship based observations. Also Price et al. (2015) found a good agreement with field data using CS-2 radar signals to derive sea-ice freeboard over the fast ice of McMurdo Sound.

Since previous studies show a proof-of-concept of hemisphere-wide sea-ice thickness retrieval using satellite altimeter time series, the next steps would be to merge data sets from different satellite missions to a consistent long-term record of Antarctic sea-ice thickness. With the radar altimeters on the ERS-1, ERS-2, Envisat and

About the consistency between Envisat and CryoSat-2 radar freeboard retrieval

S. Schwegmann et al.

Title Page

Abstract

Introduction

Conclusions

References

Tables

Figures

◀

▶

◀

▶

Back

Close

Full Screen / Esc

Printer-friendly Version

Interactive Discussion

CryoSat-2 missions of the European Space Agency, a continuous data set spanning two decades is available. One particular challenge for a merged time series though is the different radar configuration between the pulse-limited altimeters of ERS-1, ERS-2 and Envisat and CS-2, which employs along-track beam-sharpening for a smaller footprint size. As a result, the characteristics of the time-dependent radar backscatter, recorded as echo waveform for each single measurement, are inherently different in shape between the two radar altimeter acquisitions. Range retrieval from the radar waveform is often based on an empirical evaluation of the leading edge, since the full wave form of a sea-ice target is usually of high complexity. Since existing studies on freeboard or thickness are usually based on a single mission the empirical range retrieval algorithms are not necessarily consistent for different sensor types. Hence, in order to create an inter-sensor time series, we need to test different algorithms on their consistency for different sensors.

Within the ESA Climate Change Initiative (CCI) Sea ice project – Antarctic Sea-ice thickness Option – Envisat and CS-2 freeboard values over the entire Antarctic sea ice have been computed independently from each other. A freeboard time series created by those sensors has the potential to cover more than 10 years yet, from 2002 until today. More importantly, both data sets have an overlap period in 2011. This overlap is used to assess a potential inter-mission bias and sensor associated uncertainties based on independently produced monthly mean and modal freeboard values from Envisat and CS-2. Differences are discussed with respect to regional and temporal variability and potential causes are identified. We also relate the differences to the occurrence of the diverse ice classes, in which we use the terms “seasonal ice” for predominant occurrence of first year ice, perennial ice for regions with second/multi-year ice and coastal ice for all the ice (deformed drifting ice, first and multi-year ice as well as landfast ice) that occur close to the coasts. This effort is the first towards a development of consistent retrieval algorithms for both pulse-limited and beam-sharpened radar altimeters, with the objective to extend the sea-ice thickness time series in the Southern Ocean back to 1991 with ERS-1 and ERS-2.

2 Data and methods

Antarctic wide freeboard from Envisat and CS-2 data was derived by two different, sensor related processors for the overlap period in 2011. In order to distinguish between open water and sea ice, sea-ice concentration (SIC) is used in both processors. Freeboard was only derived for regions with a SIC above 55 %. Monthly mean freeboard was computed from January to December and was gridded onto a 100 km EASE-Grid 2.0 (Brodzik et al., 2012). Some comparisons are also done with a 25 km grid. The individual processors are described in Sects. 2.1 and 2.2, and Table 1 gives an overview of the most important processing parameters.

2.1 CryoSat-2 freeboard retrieval

The CS-2 freeboard processor has originally been developed for applications on Arctic sea ice and has now been adapted for the use of Antarctic sea-ice. We used the geolocated level 1b Synthetic Aperture Radar (SAR) and interferometric SAR (SARIn) waveforms over the Southern Ocean obtained from CS-2 (K_u band, 13.575 GHz) and provided by ESA (<https://earth.esa.int/web/guest/-/how-to-access-cryosat-data-6842>). The surface elevations are processed from individual CS-2 tracks using the Threshold First-Maximum Retracker Algorithm (TFMRA) described by Helm et al. (2014) and Ricker et al. (2014) in detail.

Specifically, the main scattering horizon is tracked at the leading edge of the first local maximum of the CS-2 waveform by using a power threshold (see Fig. 1). For the standard processing we used a threshold of 40 % but also tested results using a threshold of 50 % to retrieve surface elevations. Geophysical range corrections (e.g. ionospheric, tropospheric and tide corrections) are applied using the values supplied in the L1B data files of ESA. The retrieved freeboard refers to the main scattering horizon of the radar wave. As the exact position of the scattering horizon is unknown we do not apply a correction for the wave propagation speed in the snow layer. Instead we use for our calculation and comparison the freeboard from the uncorrected radar range, i.e.

About the consistency between Envisat and CryoSat-2 radar freeboard retrieval

S. Schwegmann et al.

Title Page

Abstract

Introduction

Conclusions

References

Tables

Figures

◀

▶

◀

▶

Back

Close

Full Screen / Esc

Printer-friendly Version

Interactive Discussion



we obtain the radar freeboard (F_R) instead of ice or snow freeboard:

$$F_R = L - (\text{MSSH} + \text{SSA}) \quad (1)$$

L is the retrieved surface elevation, MSSH corresponds to the mean sea-surface height product DTU10 (Andersen, 2010), which is subtracted from the surface elevations first, in order to remove the main geoid undulations. The SSA is the Sea Surface Anomaly derived from linear interpolation between elevations of detected leads along the orbit track and represents the residuum from the MSSH. The discrimination between open water (leads) and sea ice is based on the so called pulse peakiness (Eq. 2) of the return signal (Peacock and Laxon, 2004). Leads are cracks in the ice cover and usually have a distinct specular radar echo, while open-ocean and sea-ice surfaces have wider waveforms, resulting from diffuse reflection of the higher surface roughness (see Fig. 1 for comparison). The pulse peakiness (PP) is derived by

$$\text{PP} = \frac{\max(\text{WF})}{\sum_{i=1}^{N_{\text{WF}}} \text{WF}_i} \cdot N_{\text{WF}} \quad (2)$$

N_{WF} is the number of range bins and WF_i describes the echo power at range bin index i . Data points, that cannot be identified as echoes from ice, leads or open ocean are discarded due to the possibility of a range bias from off-nadir leads (snagging) (Armitage and Davidson, 2014).

Open-ocean is identified by using SIC data obtained by the Ocean and Sea Ice Satellite Application Facility (OSI SAF) High Latitude Processing Center (Eastwood, 2012) and provided on daily grids with a resolution of 10 km. SIC are interpolated onto the respective CS-2 track in order to define the ice free areas within the CS-2 freeboard processor along those tracks.

Radar freeboard lower than -0.3 m and higher than 2 m is discarded from the data sets. Indeed, negative sea-ice freeboard is possible in Antarctica, but the CS-2 signal is certainly reflected at the slush-dry snow interface. However, we allow negative freeboard to accommodate the random uncertainties caused by speckle and instrument

noise. Finally, freeboard values of all CS-2 tracks within a month are compiled and projected onto a 100 km EASE 2.0 grid for further analysis.

2.2 Envisat freeboard retrieval

The input data for the Envisat freeboard processing is the Envisat Sensor Data Record – SGDR (Sensor Geophysical Data Record) product available from ESA (https://earth.esa.int/web/guest/data-access/browse-data-products/-/asset_publisher/y8Qb/content/Envisat-sensor-data-record-1471). For the processing we used the ESA CCI RA2 prototype processor adapted for the Southern Hemisphere. The processing algorithm is described in detail on the Sea Ice CCI Algorithm Theoretical Basis Document (Ridout and Ivanova, 2012) and the prototype system in the Processing System Description (Kern, 2012).

The Envisat processing is similar to the CS-2 processing described in the Sect. 2.1. Leads are distinguished from ice floes and open water by the PP parameter. SIC information from the OSI SAF product is then used to differentiate diffuse waveforms from open water and those from ice floes. The waveforms are then retracked to retrieve the target surface elevation and radar freeboard is derived from the lead and floe elevations by interpolating the local sea level elevation measured from leads to ice floe positions and subtracting the former from the latter. As for CS-2, no correction is applied for wave propagation speed in snow so that the derived freeboard refers to the radar freeboard as well.

For Envisat we use different retrackers for leads and floes. For leads we apply the retracker described in Giles et al. (2007). The shape of a specular echo is described by two functions: the first part of the echo is represented by a Gaussian and the second part by an exponentially decaying function. These two functions are linked by a third degree polynomial function. The functions are fitted to the measured waveform using the Levenberg–Marquardt nonlinear least-squares method and one of the variables is the retracking point. For the ice floes we use a standard OCOG (offset centre of gravity) retracker with a 50 % threshold.

About the consistency between Envisat and CryoSat-2 radar freeboard retrieval

S. Schwegmann et al.

Title Page

Abstract

Introduction

Conclusions

References

Tables

Figures

◀

▶

◀

▶

Back

Close

Full Screen / Esc

Printer-friendly Version

Interactive Discussion



About the consistency between Envisat and CryoSat-2 radar freeboard retrieval

S. Schwegmann et al.

Title Page

Abstract

Introduction

Conclusions

References

Tables

Figures

◀

▶

◀

▶

Back

Close

Full Screen / Esc

Printer-friendly Version

Interactive Discussion

both data products. In summer, mean freeboard is the highest. With the beginning of the freezing season, it shows a slight decrease and over winter, it is stable and shows only a slight decrease in late spring/beginning of summer. The modal freeboard of Envisat data shows a similar seasonal cycle as mean freeboard with quite constant values over winter. CS-2 modal freeboard shows in contrast barely any variability in 2011.

A similar change from summer to winter sea-ice freeboard was found by Yi et al. (2011) analysed from ICESat data. Also Worby et al. (2008) found a similar seasonal cycle for sea-ice thicknesses obtained by ship-based observations (ASPeCt), with the highest mean thicknesses during summer and a lot thin sea ice influencing the distribution during fall. The high summer values may be caused by the quick disappearance of large areas with first year ice (FYI) in the seasonal ice zone so that the remaining perennial ice dominates the freeboard and thickness distribution. In the beginning of the freeze season, large areas are then covered by newly formed first year ice (FYI), which certainly affect the mean freeboard to decrease compared to summer values. The slight increase of mean freeboard over the growth season is in accordance with growing ice over winter. However, it may also be that a change in the penetration depth of the signal causes these high freeboard values. During summer, the location of the reflection horizon of the radar wave may be influenced by wet and/or metamorphous snow (e.g., Kwok, 2014; Willatt et al., 2010). This may lead to an apparent increase of the freeboard compared to winter data, when the radar wave potentially penetrates the snow more effectively.

There is a positive bias in the mean freeboard nearly all year round (Fig. 3a, light grey line), i.e. CS-2 freeboard is on average higher than Envisat freeboard. The highest differences occur during summer, with a maximum of 0.08 m in February. During the sea-ice growth season, between May and October, the lowest differences of about 0.01 m are found. From May to September, these differences are not statistically significant on the 95 % level. The bias for modal freeboard is instead negative all over the year and does not follow a seasonal cycle. The maximum difference for modal freeboard can be found at the end of spring, in March and April. Over the rest of the year,

it remains rather constant with values lower than or equal to 0.1 m, considering 5 cm intervals.

In order to examine whether these findings are independent from the retracker threshold difference between both processors and also from the grid resolution we modified both and analysed the results. The adaptation of the retracker threshold for CS-2 based waveforms to 50 % (Fig. 3b), as it is used for Envisat, results in higher differences for mean and modal freeboard in most months, except for summer. With an increased retracker threshold mean and modal freeboard become lower in the CS-2 data. As mean CS-2 freeboard is close to and modal freeboard mostly even lower than Envisat freeboard in the standard run, differences increase accordingly. The significance of the bias is given in winter months but not for summer months. In summer, the positive bias between CS-2 and Envisat freeboard becomes reduced in the perennial ice zone by the changed retracker threshold. The seasonal cycle of mean and modal CS-2 freeboard does not change.

An increase of the grid resolution to 25 km (retracker threshold: 40 % for CS-2, not shown) results in a similar bias for monthly mean freeboard as in the standard processing. Differences in the modal freeboard are slightly higher, similar to the processing with a retracker threshold of 50 %, in particular in the winter months.

The characteristics of the freeboard distribution, in particular the shape, have also been analysed and compared using histograms covering all grid cells of each product (Fig. 4). The distribution of the freeboard is very broad in summer and fall (January–April). From end of fall until early summer (May–December), the distribution shows a steep increase towards a distinct mode at low values and a long but flat tail towards the thicker end. The histograms show a similar shape for most months for both data sets, with Envisat freeboard (blue) slightly shifted to higher values compared to CS-2 data (black). Only during fall (March–April), the distributions differ strongly.

At the thick end of the distribution, i.e. value above 0.35 m, Envisat freeboard is less strongly represented. This issue was already visible in Fig. 2, where we could identify lower freeboard in most of the perennial ice regions. On the other hand, negative free-

About the consistency between Envisat and CryoSat-2 radar freeboard retrieval

S. Schwegmann et al.

Title Page

Abstract

Introduction

Conclusions

References

Tables

Figures

◀

▶

◀

▶

Back

Close

Full Screen / Esc

Printer-friendly Version

Interactive Discussion



board occurs more often in Envisat data than in CS-2. This is in apparent contradiction with Fig. 2, where CS-2 data show large areas covered by negative freeboard. However, these comparisons were only made for regions, where both products have valid values, i.e. large parts of the MIZ in CS-2 data were not taken into consideration in the histograms. Hence, within the pack-ice zone, Envisat data show more often negative freeboard than CS-2 data.

Figure 5 shows the regional and temporal distribution of the grid-cell based bias in monthly mean freeboard over the entire Southern Ocean. For the calculations, Envisat freeboard was subtracted from the CS-2 freeboard. Accordingly, red areas indicate that CS-2 has higher freeboard than Envisat, and blue values indicate that Envisat freeboard is higher. During winter months, the Envisat processor yields higher freeboard than CS-2 in large parts of the seasonal sea-ice zone, though in coastal regions and regions with perennial sea ice CS-2 reveal higher freeboard. In late spring, CS-2 freeboard becomes often higher than Envisat freeboard. In most regions the bias lies within ± 0.10 m, in particular between May and December. However, it can increase up to ± 0.60 m close to the coasts and in regions with predominantly perennial ice.

For the individual sectors of the Southern Ocean (following the sector classification in Parkinson and Cavalieri, 2012), the occurrence of perennial and seasonal ice has a varying impact on mean and modal freeboard (see Fig. 6). In the Weddell (WS) and Ross Seas (RS), the bias for the mean radar freeboard is negative and statistically significant over winter (April–August for WS and April–October for RS). The Ross and Weddell Seas are the regions with the largest SIE, hence, a lot of seasonal ice and free drifting sea ice far away from the coast is apparent in those sectors. Therefore, the total bias becomes negative over winter, when the area and therefore the impact of the perennial ice and the high freeboard close to the coast become less pronounced compared to the total SIE. Over summer, the percentage of those ice classes increases again and therefore, both regions show a positive, but partly not significant bias, i.e. CS-2 showing on average higher freeboard values than Envisat. In the Indian Ocean sector (IO), the Western Pacific Ocean (WPO) and in the Bellingshausen/Amundsen

About the
consistency between
Envisat and
CryoSat-2 radar
freeboard retrieval

S. Schwegmann et al.

Title Page

Abstract

Introduction

Conclusions

References

Tables

Figures

◀

▶

◀

▶

Back

Close

Full Screen / Esc

Printer-friendly Version

Interactive Discussion



About the consistency between Envisat and CryoSat-2 radar freeboard retrieval

S. Schwegmann et al.

Title Page

Abstract

Introduction

Conclusions

References

Tables

Figures

◀

▶

◀

▶

Back

Close

Full Screen / Esc

Printer-friendly Version

Interactive Discussion



Sea (ABS), either the perennial sea ice or the impact of the coastal ice dominates and leads to a year round positive bias in mean freeboard. The combination of both effects, the higher CS-2 freeboard in the perennial sea-ice zone and near the coast and the lower CS-2 freeboard in the seasonal pack-ice zone, leads to a high positive bias in summer and a nearly balanced (zero) one during winter for data averaged over the entire Antarctic sea-ice zone (see Fig. 3, left). However, the differences in the modal freeboard are for all regions for most months negative, which indicate that most of the ice-covered grid cells have higher values for Envisat data. A positive difference can be found in the IO sector (January–February), the WPO (January–February), the RS (only February) and the ABS (February–May) only in the summer months, when most of the ice is the perennial and coastal sea ice. Most of the differences for (sectional) modal freeboard are lower than or equal to ± 0.1 m (88 %), in a lot of months it is even lower than or equal to ± 0.05 m (about 57 %, considering 5 cm intervals).

4 Discussion

The present study investigates the consistency between Envisat and CS-2 radar freeboard developed independently from each other within the ESA CCI Sea ice project. We found a good agreement for the distribution of freeboard, with thicker radar freeboard in the regions with perennial ice. However, Envisat freeboard tends to be higher than CS-2 in the seasonal sea-ice zone while CS-2 data are higher compared to Envisat along the coast and in the perennial sea-ice zone. A change in the retracker threshold cannot solve this issue because this modification would change all freeboard values only in one direction: a higher leading-edge threshold would result in lower freeboard and a lower threshold in higher values. Hence, using e.g. the same retracker thresholds for both products will not improve the consistency between Envisat and CS-2 freeboard.

A potential source for inconsistencies between both data sets may be the different SSH product. For Envisat the MSSH is taken directly from the SGDR product

About the consistency between Envisat and CryoSat-2 radar freeboard retrieval

S. Schwegmann et al.

Title Page

Abstract

Introduction

Conclusions

References

Tables

Figures

◀

▶

◀

▶

Back

Close

Full Screen / Esc

Printer-friendly Version

Interactive Discussion

(ESA, 2007) file. This instead is derived from the Collecte Localisation Satellite, CLS01 monthly product (Hernandez and Schaeffer, 2000), which is referred to the EM96 geoid. The TFMRA for CS-2 freeboard calculation uses the MSSH product DTU10 (Andersen, 2010), which is a climatology and refers to the WGS84 geoid. Despite this difference, we do not expect a consequence for radar freeboard as the detection of the local SSH by lead detection in both processors should overcome the difference in the mean SSH products. Indeed, leads are expected to be sparse in the western Weddell Sea and along the coasts, because the sea ice is quite compact in those regions. However, we compared the lead densities and number of leads (see Fig. 7) for both data sets and did not find noticeable lower lead detections in regions where the differences in CS-2 and Envisat freeboard are the highest compared to regions, where the sensor biases are lower. Hence, the correction of the SSH seems not to be hampered by too few leads in the one or other data set. In future, we will nevertheless implement DTU13 consistently in both processors.

The high radar freeboard in CS-2 data along the coast may be caused by the usage of SARIn data. At the coasts, the satellite mode switches from SAR (over sea ice) to SARIn (over land ice). SARIn has generally a larger noise than the SAR data and this may lead to the higher radar freeboard in that region. However, this counts only for near-coastal grid cells and cannot explain the high radar freeboard in e.g. the western Weddell and the Amundsen/Bellingshausen Seas.

A further source for inconsistencies is certainly the difference in the sensor characteristics. The radar altimeter on-board Envisat has a much coarser resolution and lower data coverage than the one on-board CS-2. CS-2 freeboard measurements are averaged over the footprint of approximately $300\text{ m} \times 1000\text{ m}$ (Wingham et al., 2006), while Envisat data have a footprint of 2–10 km (Connor et al., 2009). A study dealing with the impact that different footprint sizes have on mean and modal freeboard in the Arctic (Schwegmann et al., 2014) showed that differences of 0.1–0.2 m for modal and 0.005 m for mean values can be expected for footprints varying from point measurements, over the ICESat footprint of 70 m to a footprint of 300 m (according to the along-track foot-

print of CS-2). Hence, a part of the difference between CS-2 and Envisat mean and modal freeboard may simply be caused by the different footprint and resolution of both measurement systems.

Also the inconsistency in SIE may be caused by the inherent difference in footprint between CS-2 and Envisat. It is likely that during the Envisat processing more data are filtered out in the MIZ because measurements from mixed ice water footprints are discarded during the processing. On the contrary, CS-2 detects more “ice only” waveforms due to the smaller footprint. As a consequence, the MIZs have not the same location in both products. Another impact factor is that in the processing of Envisat, valid ice values depend on the surrounding leads. Only if an ice value is surrounded by leads in both directions, it is valid for the freeboard processing. This criterion is not used for the CS-2 processor.

Moreover, one part of the discrepancies may be caused due to the fact that Envisat uses two individual retracker for floes and leads. For the Arctic, it was tested whether there is a possible bias in a few marginal ice zones (assuming that the actual ice freeboard of very thin ice is 0), but no bias was found. This could be different in the Antarctic, but it is not likely. However, to proof that there is no bias, an in-depth investigation of the waveforms and processor characteristics would be necessary. Such an investigation would also include a closer comparison of waveforms of the seasonal and perennial ice in order to study the causes for the biases between Envisat and CS-2 freeboard data in more detail.

The comparison done in this study cannot show how accurate freeboard measurements are and it did not aim to answer the question whether the radar altimeter signals come from the snow/ice or snow/air interface, or from somewhere in-between. A study of Price et al. (2015) indicated that the reflection horizon of CS-2 data over Antarctic sea ice, derived with a retracker threshold of 40 %, is certainly close to the snow/air interface. An adequate study of this issue is not possible at the moment of writing this paper, as there is barely any validation data published yet. However, Operation IceBridge laser freeboard measurements over Antarctic sea ice as well as laser altime-

About the consistency between Envisat and CryoSat-2 radar freeboard retrieval

S. Schwegmann et al.

Title Page

Abstract

Introduction

Conclusions

References

Tables

Figures

◀

▶

◀

▶

Back

Close

Full Screen / Esc

Printer-friendly Version

Interactive Discussion



About the consistency between Envisat and CryoSat-2 radar freeboard retrieval

S. Schwegmann et al.

Title Page

Abstract

Introduction

Conclusions

References

Tables

Figures

◀

▶

◀

▶

Back

Close

Full Screen / Esc

Printer-friendly Version

Interactive Discussion



data. Differences are mostly below 0.1 m for modal freeboard and even less for mean freeboard over winter months (May–October), although there are some inconsistencies that may be improved in future. The highest differences occur in regions with perennial sea ice and along the coasts. Nevertheless, the impact on the total Antarctic SIV is low: during the sea ice growth season, Antarctic wide SIV does only vary by few percent between Envisat and CS-2, indicating that there is a quite good consistency between both sensors. Individual sectors and summer data suffer from higher uncertainties instead, which lead to high discrepancies between the sensor-based freeboard and SIV estimates.

In order to improve the consistency between both data sets, an in-depth investigation of the waveform characteristics in both processors is needed, which was out of the scope of this study. For the future, we are however confident that this study serves – together with an improved understanding of the waveform characteristics in the pulse-limited and beam-sharpened data – as a basis for further extending the time series of sea-ice freeboard by ERS-1/2 data and compiling a sea-ice thickness time series spanning more than 20 years yet.

Acknowledgements. This research was funded by the European Space Agency Climate Change Initiative Sea ice projects SK-ESA-2012-12 and NERSC-ESA-2014-2. The work of S. Hendricks and V. Helm was funded by the German Federal Ministry of Economics and Technology (Grant 50EE1331). We would like to thank ESA, OSI SAF and DTU for providing all the data needed for freeboard processing as well as Georg Heygster and Torben Frost from the University of Bremen for providing AMSR-E snow depth.

References

Andersen, O. B.: The DTU10 Gravity field and Mean sea surface, Second international symposium of the gravity field of the Earth (IGFS2), Fairbanks, Alaska, 20–22 September 2010, 2010.

**About the
consistency between
Envisat and
CryoSat-2 radar
freeboard retrieval**

S. Schwegmann et al.

Title Page

Abstract

Introduction

Conclusions

References

Tables

Figures

◀

▶

◀

▶

Back

Close

Full Screen / Esc

Printer-friendly Version

Interactive Discussion



Armitage, T. W. K. and Davidson, M. W. J.: Using the interferometric capabilities of the ESA CryoSat-2 Mission to improve the accuracy of sea ice freeboard retrievals, *IEEE T. Geosci. Remote*, 52, 529–536, 2014.

Behrendt, A., Dierking, W., Fahrbach, E., and Witte, H.: Sea ice draft in the Weddell Sea, measured by upward looking sonars, *Earth Syst. Sci. Data*, 5, 209–226, doi:10.5194/essd-5-209-2013, 2013.

Brodzik, M. J., Billingsley, B., Haran, T., Raup, B., and Savoie, M. H.: EASE-Grid 2.0: incremental but significant improvements for earth-gridded data sets, *ISPRS Int. J. Geo-Inf.*, 1, 32–45, 2012.

Connor, L. N., Laxon, S. W., Ridout, A. L., Krabill, W. B., and McAdoo, D. C.: Comparison of Envisat radar and airborne laser altimeter measurements over Arctic sea ice, *Remote Sens. Environ.*, 113, 563–570, 2009.

Dierking, W.: Laser profiling of the ice surface-topography during the winter Weddell Gyre Study 1992, *J. Geophys. Res.-Oceans*, 100, 4807–4820, 1995.

Eastwood, S.: OSI SAF Sea Ice Product Manual, available at: <http://osisaf.met.no> (last access: 10 January 2014), 2012.

ESA: ENVISAT RA2/MWR Product Handbook, Issue 2.2, available at: https://earth.esa.int/pub/ESA_DOC/ENVISAT/RA2-MWR/ra2-mwr.ProductHandbook.2_2.pdf (last access: February 2015), 2007.

Frost, T., Heygster, G., and Kern, S.: ANT D1.1 Passive Microwave Snow Depth on Antarctic sea ice assessment, ESA-CCI Sea Ice ECV Project Report, SICCI-ANT-PMW-SDASS-11-14, ESA, available at: http://esa-cci.nersc.no/?q=webfm_send/171 (last access: 15 September 2015), 2014.

Giles, K. A., Laxon, S. W., Wingham, D. J., Wallis, D. W., Krabill, W. B., Leuschen, C. J., McAdoo, D., Manizade, S. S., and Raney, R. K.: Combined airborne laser and radar altimeter measurements over the Fram Strait in May 2002, *Remote Sens. Environ.*, 111, 182–194, 2007.

Giles, K. A., Laxon, S. W., and Worby, A. P.: Antarctic sea ice elevation from satellite radar altimetry, *Geophys. Res. Lett.*, 35, L03503, doi:10.1029/2007GL031572, 2008.

Haas, C.: Evaluation of ship-based electromagnetic-inductive thickness measurements of summer sea-ice in the Bellingshausen and Amundsen Seas, Antarctica, *Cold Reg. Sci. Technol.*, 27, 1–16, 1998.

- Haas, C., Nicolaus, M., Willmes, S., Worby, A., and Flinspach, D.: Sea ice and snow thickness and physical properties of an ice floe in the western Weddell Sea and their changes during spring warming, *Deep-Sea Res. Pt. II*, 55, 963–974, 2008.
- Harms, S., Fahrbach, E., and Strass, V. H.: Sea ice transports in the Weddell Sea, *J. Geophys. Res.-Oceans*, 106, 9057–9073, 2001.
- Helm, V., Humbert, A., and Miller, H.: Elevation and elevation change of Greenland and Antarctica derived from CryoSat-2, *The Cryosphere*, 8, 1539–1559, doi:10.5194/tc-8-1539-2014, 2014.
- Hernandez, F. and Schaeffer, P.: Altimetric Mean Sea Surfaces and Gravity Anomaly maps inter-comparisons, AVI-NT-011-5242-CLS, CLS, Ramonville St Agne, 2000.
- Kern, S.: Sea Ice Climate Change Initiative Phase 1, Product Specification Document, ESA Document, Doc Ref: SICCI-PSD-02-12, ESA, available at: http://esa-cci.nersc.no/?q=webfm_send/153 (last access: 15 September 2015), 2012.
- Kern, S. and Spreen, G.: Uncertainties in Antarctic sea-ice thickness retrieval from ICESat, *Ann. Glaciol.*, 56, 107–119, 2015.
- Kern, S., Frost, T., and Heygster, G.: ANT D1.3 Product User Guide (PUG) for Antarctic Snow Depth product SD v1.0, ESA-CCI Sea Ice ECV Project Report, SICCI-ANT-SD-PUG-14-08, ESA, available at: http://icdc.zmaw.de/fileadmin/user_upload/ESA_Sea-Ice-ECV/SICCI_ANT_SIT_Option_PUG_D1.3_Issue_2.1_final.pdf (last access: 15 September 2015), 2014.
- Kurtz, N. T., Galin, N., and Studinger, M.: An improved CryoSat-2 sea ice freeboard retrieval algorithm through the use of waveform fitting, *The Cryosphere*, 8, 1217–1237, doi:10.5194/tc-8-1217-2014, 2014.
- Kwok, R.: Simulated effects of a snow layer on retrieval of CryoSat-2 sea ice freeboard, *Geophys. Res. Lett.*, 41, 5014–5020, 2014.
- Lange, M. A. and Eicken, H.: The sea ice thickness distribution in the Northwestern Weddell Sea, *J. Geophys. Res.-Oceans*, 96, 4821–4837, 1991.
- Laxon, S. W., Giles, K. A., Ridout, A. L., Wingham, D. J., Willatt, R., Cullen, R., Kwok, R., Schweiger, A., Zhang, J. L., Haas, C., Hendricks, S., Krishfield, R., Kurtz, N., Farrell, S., and Davidson, M.: CryoSat-2 estimates of Arctic sea ice thickness and volume, *Geophys. Res. Lett.*, 40, 732–737, 2013.
- Leuschen, C. J., Swift, R. N., Comiso, J. C., Raney, R. K., Chapman, R. D., Krabill, W. B., and Sonntag, J. G.: Combination of laser and radar altimeter height measurements to estimate

About the consistency between Envisat and CryoSat-2 radar freeboard retrieval

S. Schwegmann et al.

Title Page	
Abstract	Introduction
Conclusions	References
Tables	Figures
◀	▶
◀	▶
Back	Close
Full Screen / Esc	
Printer-friendly Version	
Interactive Discussion	



**About the
consistency between
Envisat and
CryoSat-2 radar
freeboard retrieval**

S. Schwegmann et al.

Title Page

Abstract

Introduction

Conclusions

References

Tables

Figures

◀

▶

◀

▶

Back

Close

Full Screen / Esc

Printer-friendly Version

Interactive Discussion

snow depth during the 2004 Antarctic AMSR-E Sea Ice field campaign, *J. Geophys. Res.-Oceans*, 113, C04S90, doi:10.1029/2007JC004285, 2008.

Lindsay, R. and Schweiger, A.: Arctic sea ice thickness loss determined using subsurface, aircraft, and satellite observations, *The Cryosphere*, 9, 269–283, doi:10.5194/tc-9-269-2015, 2015.

Ozsoy-Cicek, B., Ackley, S., Xie, H. J., Yi, D. H., and Zwally, J.: Sea ice thickness retrieval algorithms based on in situ surface elevation and thickness values for application to altimetry, *J. Geophys. Res.-Oceans*, 118, 3807–3822, 2013.

Parkinson, C. L. and Cavalieri, D. J.: Antarctic sea ice variability and trends, 1979–2010, *The Cryosphere*, 6, 871–880, doi:10.5194/tc-6-871-2012, 2012.

Peacock, N. R. and Laxon, S. W.: Sea surface height determination in the Arctic Ocean from ERS altimetry, *J. Geophys. Res.-Oceans*, 109, C07001, doi:10.1029/2001JC001026, 2004.

Perovich, D. K., Elder, B. C., Claffey, K. J., Stammerjohn, S., Smith, R., Ackley, S. F., Krouse, H. R., and Gow, A. J.: Winter sea-ice properties in Marguerite Bay, Antarctica, *Deep-Sea Res. Pt. II*, 51, 2023–2039, 2004.

Price, D., Beckers, J., Ricker, R., Kurtz, N., Rack, W., Haas, C., Helm, V., Hendricks, S., Leanoard, G., and Langhorne, P. J.: Evaluation of CryoSat-2 derived sea-ice freeboard over fast ice in McMurdo Sound, Antarctica, *J. Glaciol.*, 61, 285–300, 2015.

Ricker, R., Hendricks, S., Helm, V., Skourup, H., and Davidson, M.: Sensitivity of CryoSat-2 Arctic sea-ice freeboard and thickness on radar-waveform interpretation, *The Cryosphere*, 8, 1607–1622, doi:10.5194/tc-8-1607-2014, 2014.

Ridout, A. and Ivanova, N.: Sea Ice Climate Change Initiative Phase 1, Algorithm Theoretical Basis Document (ATBDv0) issue 1.1, ESA Document, Doc Ref: SICCI-ATBDv0-07-12, ESA, available at: http://esa-cci.nersec.no/?q=webfm_send/160 (last access: 15 September 2015), 2012.

Rothrock, D. A., Yu, Y., and Maykut, G. A.: Thinning of the Arctic sea-ice cover, *Geophys. Res. Lett.*, 26, 3469–3472, 1999.

Rothrock, D. A., Percival, D. B., and Wensnahan, M.: The decline in Arctic sea-ice thickness: separating the spatial, annual, and interannual variability in a quarter century of submarine data, *J. Geophys. Res.-Oceans*, 113, C05003, doi:10.1029/2007JC004252, 2008.

Schwegmann, S., Hendricks, S., Haas, C., and Herber, A.: Effects of different footprint areas on the comparability between measurements of sea ice freeboard, IGS International

**About the
consistency between
Envisat and
CryoSat-2 radar
freeboard retrieval**

S. Schwegmann et al.

Title Page

Abstract

Introduction

Conclusions

References

Tables

Figures

◀

▶

◀

▶

Back

Close

Full Screen / Esc

Printer-friendly Version

Interactive Discussion



Symposium on Sea Ice in a Changing Environment, Hobart, Tasmania, Australia, 10–14 March 2014, available at: <http://epic.awi.de/35386/> (last access: February 2015), 2014.

Wadhams, P., Lange, M. A., and Ackley, S. F.: The ice thickness distribution across the Atlantic sector of the Antarctic Ocean in midwinter, *J. Geophys. Res.-Oceans*, 92, 14535–14552, 1987.

Weissling, B. P., Lewis, M. J., and Ackley, S. F.: Sea-ice thickness and mass at Ice Station Belgica, Bellingshausen Sea, Antarctica, *Deep-Sea Res. Pt. II*, 58, 1112–1124, 2011.

Willatt, R., Laxon, S., Giles, K., Cullen, R., Haas, C., and Helm, V.: Ku-band radar penetration into snow cover Arctic sea ice using airborne data, *Ann. Glaciol.*, 52, 197–205, 2011.

Willatt, R. C., Giles, K. A., Laxon, S. W., Stone-Drake, L., and Worby, A. P.: Field investigations of Ku-Band radar penetration into snow cover on Antarctic sea ice, *IEEE T. Geosci. Remote*, 48, 365–372, 2010.

Wingham, D. J., Francis, C. R., Baker, S., Bouzinac, C., Brockley, D., Cullen, R., de Chateau-Thierry, P., Laxon, S. W., Mallow, U., Mavrocordatos, C., Phalippou, L., Ratier, G., Rey, L., Rostan, F., Viau, P., and Wallis, D. W.: CryoSat: a mission to determine the fluctuations in Earth's land and marine ice fields, *Adv. Space Res.*, 37, 841–871, 2006.

Worby, A. P., Geiger, C. A., Paget, M. J., Van Woert, M. L., Ackley, S. F., and DeLiberty, T. L.: Thickness distribution of Antarctic sea ice, *J. Geophys. Res.-Oceans*, 113, C05S92, doi:10.1029/2007JC004254, 2008.

Xie, H., Ackley, S. F., Yi, D., Zwally, H. J., Wagner, P., Weissling, B., Lewis, M., and Ye, K.: Sea-ice thickness distribution of the Bellingshausen Sea from surface measurements and ICESat altimetry, *Deep-Sea Res. Pt. II*, 58, 1039–1051, 2011.

Yi, D. H., Zwally, H. J., and Robbins, J. W.: ICESat observations of seasonal and interannual variations of sea-ice freeboard and estimated thickness in the Weddell Sea, Antarctica (2003–2009), *Ann. Glaciol.*, 52, 43–51, 2011.

Zwally, H. J., Yi, D. H., Kwok, R., and Zhao, Y. H.: ICESat measurements of sea ice freeboard and estimates of sea ice thickness in the Weddell Sea, *J. Geophys. Res.-Oceans*, 113, C02S15, doi:10.1029/2007JC004284, 2008.

About the consistency between Envisat and CryoSat-2 radar freeboard retrieval

S. Schwegmann et al.

Table 2. Sea-ice volume (SIV) in km^3 calculated from CS-2 and Envisat radar freeboard with AMSR-E snow depth information (Frost et al., 2014; Kern et al., 2014) for three test cases, depending on the location of the radar wave's main scattering horizon: (a) location 5 cm below the snow surface, (b) location 15 cm below the snow surface, (c) location at the ice/snow interface. Data are only listed until September because AMSR-E snow depth information is not available beyond September 2011. Bold numbers show where the difference between CS-2 and Envisat SIV is lower than 2%. Negative values occur when the apparent snow freeboard (radar freeboard + correction for wave propagation speed + assumed snow above main scattering horizon) is lower than the actual snow depth. That means that the assumed location of the main scattering horizon is certainly not realistic in those cases.

SIV (km^3)	CS-2 (a)	Envisat (a)	CS-2 (b)	Envisat (b)	CS-2 (c)	Envisat (c)
Jan	−113.5	−953.7	1451.3	611.1	5937.1	5096.9
Feb	44.6	−922.0	1479.4	512.7	5790.1	4823.4
Mar	1829.8	886.2	3407.4	2463.8	6649.1	5705.5
Apr	3808.8	2817.0	6073.5	5081.7	9301.4	8309.6
May	6890.2	6983.8	12 642.0	12 735.5	16 553.6	16 647.1
Jun	7899.8	8191.5	16 455.9	16 747.6	23 550.5	23 842.2
Jul	7433.3	7072.1	18 830.4	18 469.2	31 860.0	31 498.9
Aug	10 930.4	10 870.7	23 436.1	23 376.3	35 775.1	35 715.4
Sep	12 820.3	12 143.6	25 606.2	24 929.4	36 940.0	36 263.2

Title Page

Abstract

Introduction

Conclusions

References

Tables

Figures

◀

▶

◀

▶

Back

Close

Full Screen / Esc

Printer-friendly Version

Interactive Discussion



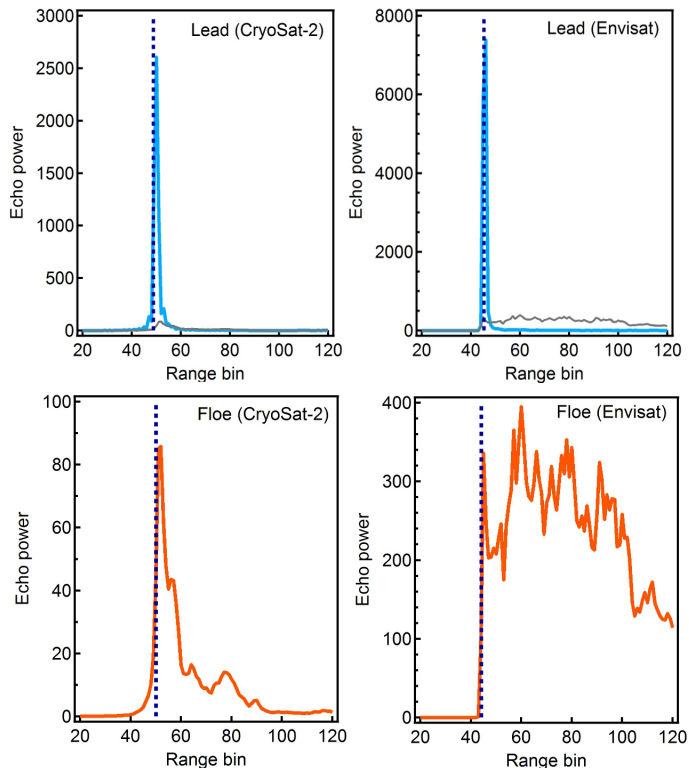


Figure 1. Waveform example for a lead (top) and a floe (bottom) for CS-2 (left) and Envisat (right). Blue dashed lines show the retracking point of each waveform. Notice the different scales on the y axis: lead detections have a much higher echo power and a steeper leading edge than waveforms originating from ice only detections. To make the different echo powers better visible, the floe waveforms are shown in the upper figures (leads) in grey. Waveforms from CS-2 and Envisat do not originate from the same position but show rather an arbitrary example.

About the consistency between Envisat and CryoSat-2 radar freeboard retrieval

S. Schwegmann et al.

Title Page

Abstract Introduction

Conclusions References

Tables Figures

◀ ▶

◀ ▶

Back Close

Full Screen / Esc

Printer-friendly Version

Interactive Discussion



About the
consistency between
Envisat and
CryoSat-2 radar
freeboard retrieval

S. Schwegmann et al.

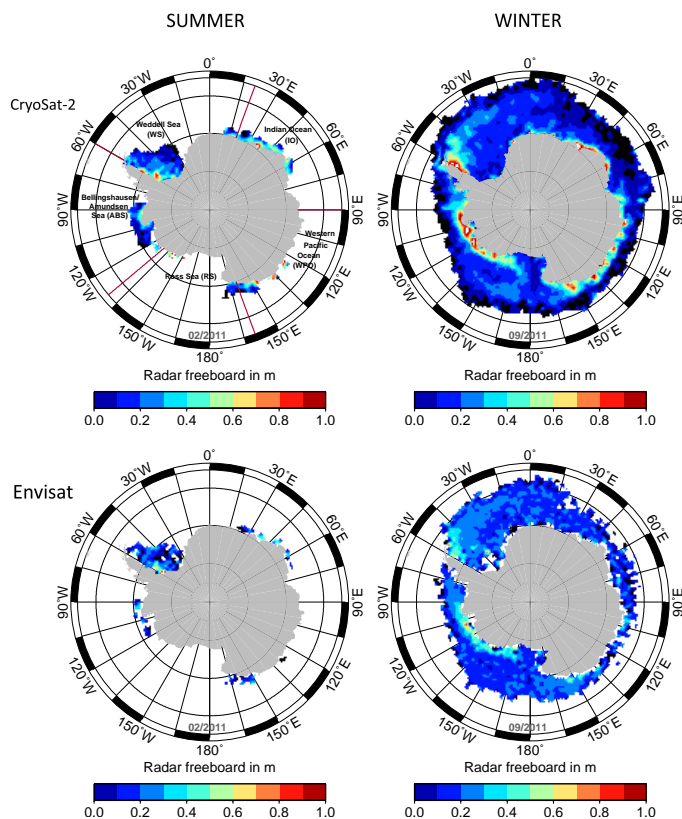


Figure 2. Freeboard distribution from CS-2 (top) and Envisat (bottom), exemplarily for sea-ice minimum in summer (left) and maximum in winter (right). Black areas show regions with negative radar freeboard. Upper left image also includes the definition of the individual sectors after Parkinson and Cavalieri (2012).

Title Page

Abstract

Introduction

Conclusions

References

Tables

Figures

◀

▶

◀

▶

Back

Close

Full Screen / Esc

Printer-friendly Version

Interactive Discussion

About the consistency between Envisat and CryoSat-2 radar freeboard retrieval

S. Schwegmann et al.

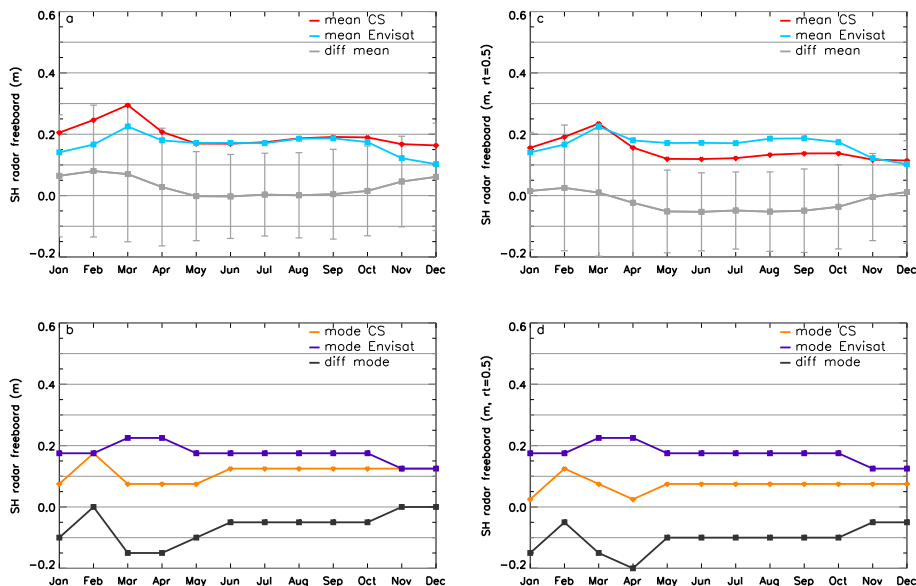


Figure 3. Seasonal cycle of mean (a, c) and modal (b, d) freeboard from CS-2 and Envisat data as well as difference between them (CryoSat-2 – Envisat) for the standard processing (left) and CS-2 processing with retracker threshold of 50 % (right). Grey bars show standard deviation of differences. Data have been averaged over the entire Antarctic sea-ice zone covered by at least 55 % sea ice, but only where both data products have a valid value.

Title Page

Abstract

Introduction

Conclusions

References

Tables

Figures

◀

▶

◀

▶

Back

Close

Full Screen / Esc

Printer-friendly Version

Interactive Discussion

About the
consistency between
Envisat and
CryoSat-2 radar
freeboard retrieval

S. Schwegmann et al.

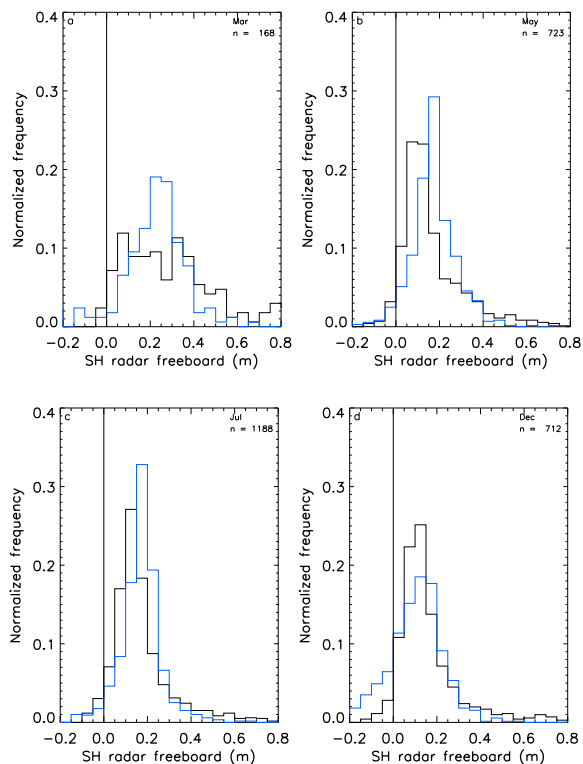


Figure 4. Histograms of freeboard distribution for CS-2 (black) and Envisat (blue) data, exemplarily for March and May (fall), July (winter) and December (summer). Only data occurring in both data sets have been considered. n is the number of compared grid cells.

Title Page

Abstract

Introduction

Conclusions

References

Tables

Figures

◀

▶

◀

▶

Back

Close

Full Screen / Esc

Printer-friendly Version

Interactive Discussion

About the
consistency between
Envisat and
CryoSat-2 radar
freeboard retrieval

S. Schwegmann et al.

Title Page

Abstract

Introduction

Conclusions

References

Tables

Figures

◀

▶

◀

▶

Back

Close

Full Screen / Esc

Printer-friendly Version

Interactive Discussion

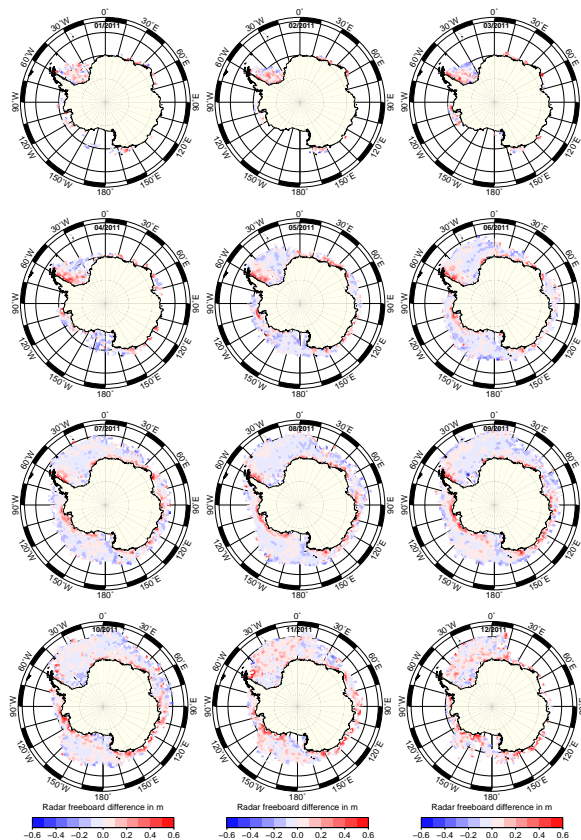


Figure 5. Difference between CS-2 and Envisat (CryoSat-2 – Envisat) freeboard. Blue colours indicate that Envisat freeboard is higher than CS-2 freeboard and red colours indicate that CS-2 freeboard is higher.

About the consistency between Envisat and CryoSat-2 radar freeboard retrieval

S. Schwegmann et al.

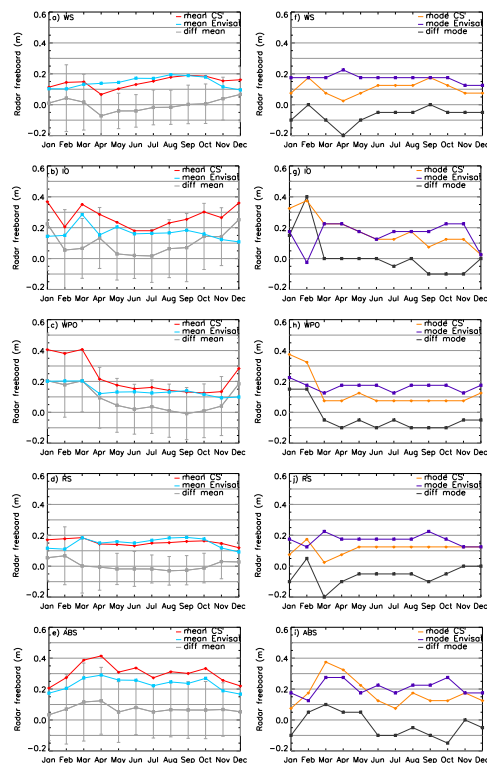


Figure 6. Mean (a–e) and modal (f–j) freeboard averaged for the Weddell Sea (WS), Indian Ocean sector (IO), Western Pacific Ocean (WPO), Ross Sea (RS) and Amundsen/Bellingshausen Seas (ABS). Grey curves show the mean and modal differences between both sensors (CryoSat-2 – Envisat) and attached bars show the standard deviation of differences. Only data occurring in both data sets have been considered.

Title Page

Abstract

Introduction

Conclusions

References

Tables

Figures

◀

▶

◀

▶

Back

Close

Full Screen / Esc

Printer-friendly Version

Interactive Discussion

About the
consistency between
Envisat and
CryoSat-2 radar
freeboard retrieval

S. Schwegmann et al.

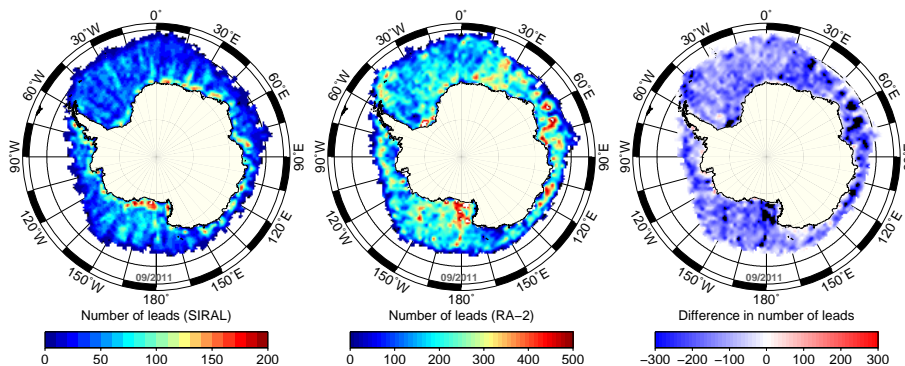


Figure 7. Number of lead detections per grid cell for CS-2 (left) and Envisat (middle) and the difference CS-2 – Envisat (right). Blue values in the right-hand figure indicate that within a grid cell, for Envisat more waveforms are classified as leads than for CS-2.

Title Page

Abstract

Introduction

Conclusions

References

Tables

Figures

◀

▶

◀

▶

Back

Close

Full Screen / Esc

Printer-friendly Version

Interactive Discussion

About the
consistency between
Envisat and
CryoSat-2 radar
freeboard retrieval

S. Schwegmann et al.

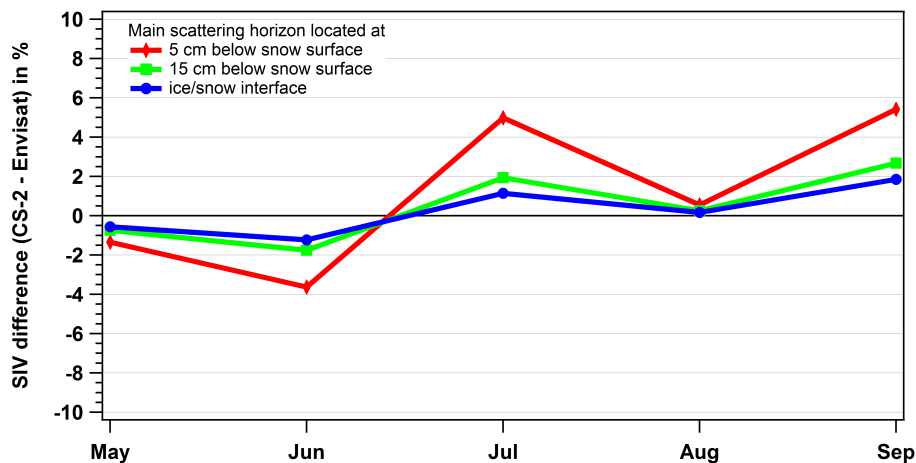


Figure 8. Sea ice volume (SIV) difference (CS-2 – Envisat) over the sea ice growth season related to the averaged sea ice volume derived from CS-2 and Envisat. Since the location of the wave’s main scattering horizon is unknown, we tested different cases (location 5 and 15 cm below the snow surface and location at ice/snow interface).

Title Page

Abstract

Introduction

Conclusions

References

Tables

Figures

◀

▶

◀

▶

Back

Close

Full Screen / Esc

Printer-friendly Version

Interactive Discussion